ORIGINALARBEITEN/ORIGINALS

Simulation Study on the Tribological Characteristics in the Meshing Contact in the Context of the Load Carrying Capacity Calculation of Internal Gears with Unbalanced Sliding Conditions

Michael Geitner[1] · Sebastian Preintner[1] · Thomas Tobie[1] · Karsten Stahl[1]

Abstract

Planetary gearboxes are characterized by a high power density and a compact design with coaxial in- and output. Consequently, planetary gear units are frequently used in many practical applications, e.g. in wind energy and industrial transmission systems as well as in automotive applications such as automatic transmissions. As a result of the scaling-up of the required system power, the risk of flank damages increased during the last decade. Certain damage types, such as pitting and micropitting, occur predominantly in contact areas of negative specific sliding on the tooth flank surface. Unlike external gears, internal gears offer the possibility of positioning the pitch point C outside of the active profile. Depending on the gear design, this allows a complete avoidance of negative specific sliding either on the planet or on the ring gear. In contrast, the corresponding gear is subjected to negative specific sliding only. It can be assumed that the lifetime regarding flank damages of each meshing partner can be affected by different positions of the pitch point and the resulting differences in the specific sliding, which allows an optimization of the full gear system, taking into account e.g. the load carrying capacity reserves for different material pairings. It is to be noted that such gear designs are already part of some practical applications.

However, the existing analytical approaches within standardized load carrying capacity calculation methods are typically based on investigations considering external gears with balanced sliding conditions. Systematic results on internal gear designs with pitch point positioned outside of the active profile are not available.

Within this paper, extended theoretical studies on the tribological characteristics of different internal gear designs are presented. Therefore, a reference geometry with balanced sliding conditions is compared to internal gears with pitch point below respectively above the active profile. The focus of the studies is the analysis of the lubricant film thickness and the contact temperature in the meshing contact. Referring to this, a high-order TEHL contact simulation model was used. The results of the numerical analysis with the FZG calculation software TriboMesh are compared to different analytical approaches in the context of the calculation of load carrying capacity to derive recommendations for the design of internal gears.

✉ Michael Geitner
   michael.geitner@tum.de

   Sebastian Preintner
   sebastian.preintner@tum.de

   Thomas Tobie
   thomas.tobie@tum.de

   Karsten Stahl
   karsten.stahl@tum.de

[1] Gear Research Center (FZG), Technical University of Munich, Garching, Germany

Berechnungsstudie hinsichtlich der für die Zahnradtragfähigkeit relevanten tribologischen Eigenschaften im Zahnkontakt von Innenverzahnungen mit unausgeglichenen Gleitverhältnissen

Zusammenfassung

Planetengetriebe zeichnen sich durch eine hohe Leistungsdichte und eine kompakte Bauweise mit koaxialem Ein- und Ausgang aus. Daher werden Planetengetriebe häufig in vielen praktischen Anwendungen eingesetzt, z. B. in Windenergie- und Industriegetrieben sowie in Automobilanwendungen wie Automatikgetrieben. Infolge der Erhöhung der erforderlichen Systemleistung ist das Risiko von Flankenschäden im letzten Jahrzehnt angestiegen. Bestimmte Schadensarten, wie Grübchen und Graufleckigkeit, treten vorwiegend in Kontaktbereichen mit negativem spezifischem Gleiten auf der Zahnflankenoberfläche auf. Im Gegensatz zu Außenverzahnungen bieten Innenverzahnungen die Möglichkeit, den Wälzpunkt C außerhalb der Eingriffsstrecke zu positionieren. Dadurch kann je nach Auslegung des Zahnrades negatives spezifisches Gleiten entweder auf dem Planeten oder auf dem Hohlrad vollständig vermieden werden. Im Gegensatz dazu ist das entsprechende Gegenrad auschließlich negativem spezifischem Gleiten ausgesetzt. Es ist davon auszugehen, dass die Lebensdauer hinsichtlich der Flankenschäden der einzelnen Wälzpartner durch unterschiedliche Lage des Wälzpunktes und den daraus resultierenden Unterschieden im spezifischen Gleiten beeinflusst werden kann, was eine Optimierung des gesamten Getriebesystems, z.B. unter Berücksichtigung der Tragfähigkeitsreserven für unterschiedliche Werkstoffpaarungen, ermöglicht. Es ist anzumerken, dass solche Getriebeauslegungen bereits in einigen praktischen Anwendungen zu finden sind.

Die vorhandenen analytischen Ansätze innerhalb standardisierter Tragfähigkeitsberechnungsmethoden basieren jedoch typischerweise auf Untersuchungen an Außenverzahnungen mit ausgeglichenen Gleitverhältnissen. Systematische Ergebnisse zu Innenverzahnungen, bei denen der Wälzpunkt außerhalb der Eingriffsstrecke liegt, liegen nicht vor.

In dieser Arbeit werden erweiterte theoretische Untersuchungen zu den tribologischen Eigenschaften verschiedener Innenverzahnungen vorgestellt. Dazu wird eine Referenzgeometrie mit ausgeglichenen Gleitverhältnissen mit Innenverzahnungen verglichen, bei denen der Wälzpunkt vor bzw. nach der Eingriffsstrecke liegt. Der Schwerpunkt der Untersuchungen liegt auf der Analyse der Schmierfilmdicke und der Kontakttemperatur im Zahneingriff. Hierfür wurde ein TEHL-Kontaktsimulationsmodell höherer Ordnung verwendet. Die Ergebnisse der numerischen Analyse mit der FZG-Berechnungssoftware TriboMesh werden in Bezug auf die Tragfähigkeitsberechnung mit verschiedenen analytischen Ansätzen verglichen, um daraus Empfehlungen für die Auslegung von Innenverzahnungen abzuleiten.

1 Introduction

Due to a high power density and a compact design with coaxial in- and output, planetary gear stages are often part of transmission systems in the practical application. In the last decade, the requirements and transmittable power increased, e.g. in wind energy and industrial transmission systems as well as in automotive applications such as automatic transmissions. Correspondingly, the risk of flank damages enhanced. For certain damage types, such as pitting and micropitting, the damage occurrence predominantly is located in contact areas of negative specific sliding on the tooth flank surface.

In contrast to external gears, internal gears offer the possibility to position the pitch point C outside of the active profile. Thereby, negative specific sliding can be completely avoided for either planet or ring gear, while the corresponding gear is subjected to negative specific sliding only. Furthermore, the values of the negative specific sliding can be reduced. By an adequate positioning of the pitch point C, it is assumed that the flank load carrying capacity of gears can be specifically influenced due to the resulting direction and values of the specific sliding. Taking into account

e.g. the load carrying capacity reserves for different material pairings, this allows an optimization of the full gear system.

Although such gear designs are already applied in practice, results of systematic investigations on internal gears with unbalanced sliding conditions are not available yet. The flank load carrying capacity reserves of materials in the areas of positive specific sliding are not quantified and existing calculation methods are not verified for internal gears with the pitch point C positioned outside of the active profile.

A calculation study on the tribological characteristics, which influence the flank load carrying capacity, in the gear meshing contact of internal gears is presented within this paper. To investigate the influence of the sliding conditions, three internal gear geometries are compared, including a reference geometry with balanced sliding conditions and two designs with pitch point C below respectively above the active profile. Comparable loading conditions are defined under systemtic variation of the contact pressure and circumferential speed, which the lubricant film thickness and the contact temperature in the meshing contact are analyzed for. Since available analytical approaches are derived

and validated typically from investigations on external gear geometries with balanced sliding conditions, a high-order TEHL contact simulation model is used. The results of the numerical analysis are compared to different analytical approaches in the context of the calculation of load carrying capacity. Finally, several considerations for internal gears with unbalanced sliding conditions are derived from the results of the simuation study.

2 Gear geometry, specific sliding and definded loading conditions

2.1 Gear geometry and properties

As reference model with balanced sliding conditions, the well-established FZG internal spur gear [22] is used within the theoretical investigations. To analyze the influence of unbalanced sliding conditions, two internal gear geometries with the pitch point C below respectively above the active profile were designed, generally with a comparable number of teeth respectively transmission ratio and a fixed center distance. As all gear geometries are designed to be also tested experimentally within the FZG internal gear test rig [11], certain dimension restrictions, such as e.g. maximum tip diameters, are considered consequently. With a normal module of $m_n = 4.0$ mm, the two variants C below and C above have a comparable size to the reference geometry ($m_n = 4.5$ mm). The calculated transverse contact ratio ε_α as well as the active profile length g_α of the variants C below and C above are almost identical, but slightly lower compared to the reference. Fig. 1 shows the main

gear data of the planets and the ring gears. Within the theoretical investigations, both the planet and ring gears are assumed to be made from case-hardened steel (with Young's modulus = 206,000 MPa, Poisson's ratio $v = 0.3$ and material density $\varrho = 7760$ kg/m³).

2.2 Specific sliding

Assumed within the theoretical investigations, the planet gear drives the ring gear. Consequently, the beginning of contact (point A) for the gear pairing is located in the dedendum flank area of the planet respectively in the addendum flank area of the ring gear. In Fig. 2, the sliding conditions within the active profile are illustrated by the specific sliding ζ, a dimensionless parameter, which is only depending on the gear geometry (gear pairing i and j) and can be calculated for each gearing partner in the contact point (Y) by the ratio of occurring sliding speed v_{slipYi} and tangential speed v_{tanYi} (see Eq. 1).

$$\xi_i = \frac{v_{\text{slipY}i}}{v_{\text{tanY}i}} = \frac{v_{\text{tanY}i} - v_{\text{tanY}j}}{v_{\text{tanY}i}} = 1 - \frac{\rho_{Yj}}{\rho_{Yi}} \cdot \frac{z_i}{z_j}. \quad (1)$$

The reference gear geometry (blue) with the pitch point C approximately central on the active profile is characterized by balanced sliding conditions, i.e. negative specific sliding for the planet between A and C, positive specific sliding between C and E respectively vice versa for the ring gear. The variant with the pitch point C below the active profile (green) shows only positive specific sliding on the planet gear over the entire meshing distance A to E and exclusively negative specific sliding on the ring gear.

Fig. 1 Gear data of the investigated internal gears

| Parameter	Unit	Reference (Ref)		C below		C above	
		Planet	Ring gear	Planet	Ring gear	Planet	Ring gear
Normal module m_n	mm	4.5		4.0		4.0	
Number of teeth z	-	16	-42	17	-47	18	-43
Common face width b	mm	8.0					
Pressure angle α_n	°	20					
Helix angle β	°	0					
Transverse contact ratio ε_α	-	1.437		1.230		1.221	
Addendum modification coefficient x	-	0.1817	-0.2963	0.5332	-0.3000	0.4708	-3.7350
Tip circle diameter d_a	mm	82.45	-185.0	80.65	-185.0	82.65	.185.0
Addendum active profile length $g_{\alpha\alpha}$	mm	10.375	8.715	14.771	-0.225	-1.958	16.374
Center distance a	mm	-59.0					
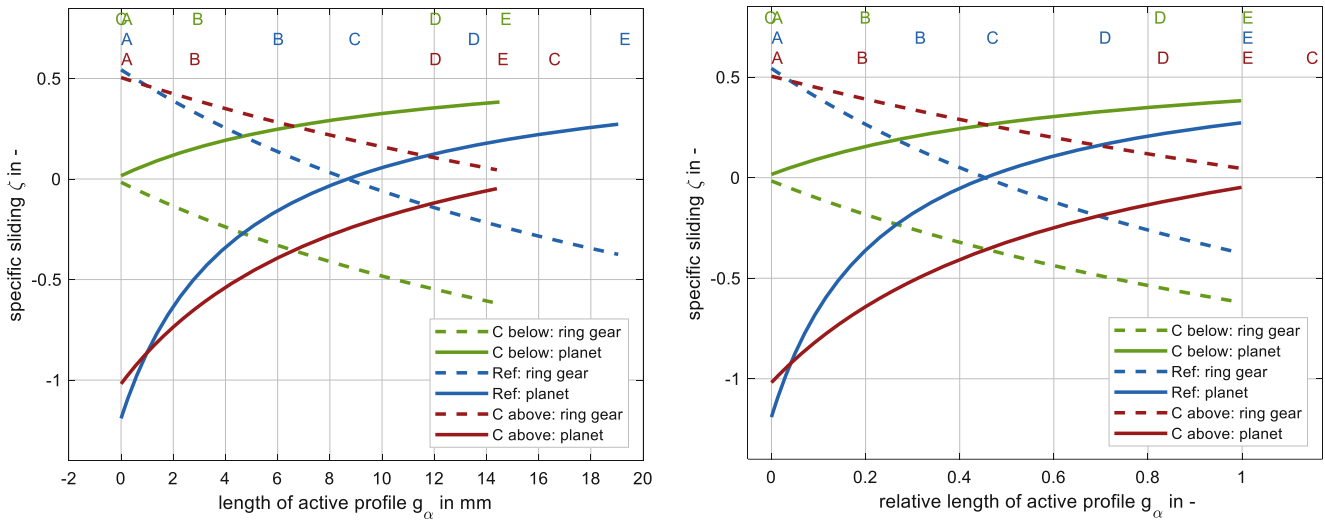
Fig. 2 Specific sliding over the (*left*: absolute, *right*: relative) length of active profile for the investigated internal gear geometries (see Fig. 1)

If the pitch point is above the active profile (C above, red), the gear geometry shows only negative specific sliding on the planet and only positive specific sliding on the ring gear. The maximum of the specific sliding is generally comparable for all variants and designed in a common and adequate range (i.a. to avoid scuffing), only variant C below is characterized by somewhat decreased values. While Fig. 2 shows a comparison also over the relative length of active profile for reasons of the comparability of the variants (right), the illustrations in this paper mainly consider the absolute length of active profile due to its significant influence on the investigated parameters.

2.3 Defined operating conditions for simulation

The load stage test according to [20] (based on the micropitting test according to FVA 54/7 [8] respectively DIN 3990-16 [1]) serves as base of the defined loading conditions (pairing hard/hard considered). Here, values of the Hertzian

pressure p_C at the pitch point C are specified in the test procedure. For the variants with C outside of the active profile, a corresponding nominal load cannot be transferred directly, since the pitch point represents only a virtual point of contact. For this reason, the maximum occurring Hertzian pressure $p_{H,max}$ was used as a comparable parameter within the investigations. Particularly for the variants with the pitch point C outside the active profile, it is assumed that load carrying capacity depends to a large extent on the maximum pressure that occurs, since there is uniform specific sliding direction over the contact area.

First (see Fig. 3, step 1), the torque T_{Ref} was determined for the reference geometry, defined by the required pressure in the pitch point C per load stage (BS, see [20]). Analogously to the procedure in [10, 26], the influence of the load distribution in the direction of the face width was taken into

Fig. 3 Defined load stages and test torques

BS	$p_C{}^*$ in N/mm² (defined in [26])	T_{pl} in Nm (Ref)	$p_{H,max}$ in N/mm² (from RIKOR)	T_{pl} in Nm (C below)	T_{pl} in Nm (C above)
6	800	98.5	992	144.8	115.1
7	950	140.2	1151	196.4	155.3
8	1100	188.1	1269	239.4	189.2
9	1250	245.1	1446	312.3	246.1
10	1400	307.4	1617	391.4	308.4
11	1550	376.9	1788	479.6	377.2

account by means of the face load factor $K_{H\beta}$ (contact stress) according to ISO 6336-1 [3] additionally (see Eq. 2).

$$p_C{}^* = p_C \cdot \sqrt{K_{H\beta}}. \qquad (2)$$

The factor $K_{H\beta}$ was therefore calculated depending on the applied loading on the internal gears using the FZG calculation program RIKOR (see also [7]), under consideration i.a. of the deformations within the shaft-bearing-system of the FZG internal gear test rig.

As result of the RIKOR calculations, the maximum occurring Hertzian pressure $p_{H,max}$ could be specified in each load stage and defined as a new characteristic load parameter (see Fig. 3, step 2). Here, effects due to a premature contact were not taken into account. It is to be noted that, based on the practical application and in accordance with manufactured test gears for comparable experimental investigations (not part of this paper), a short tip relief of $C_a = 35\,\mu m$ for all planet and ring gears was considered in the RIKOR calculations.

With the same values of the maximum occurring Hertzian pressure $p_{H,max}$ as comparable parameter per load stage, the corresponding torque for the variants C below and C above was derived from further RIKOR simulations (see Fig. 3, step 3). Fig. 3 shows stepwise the procedure of defining the loading conditions, and gives an overview of the loads and test torques per load stage.

Besides the variation of the applied load (BS 6–11), three different circumferential speeds are considered within the calculation study. Based on former investigations [10, 11, 22], $v_t = 2.0\,m/s$ as well as reduced speeds of $0.5\,m/s$ and $0.05\,m/s$ (defined in the pitch point C) represent relevant operating conditions, which can be critical for gears regarding micropitting and wear due to a small occurring lubricant film thickness in the gear contact.

The tooth mesh is assumed to be lubricated by research reference oil FVA 3A (mineral oil with 4% Anglamol 99,

ISO VG 100) with injection lubrication at $\vartheta_{oil} = 60\,°C$. The specific lubricant data (incl. empiric factors for different analytical approaches deduced from regression analysis) are described in [4, 12, 14], a summary can be found in [18].

3 TEHL contact simulation

3.1 TEHL contact

Fig. 4 schematically shows the contraform TEHL contact of two convex contact bodies [6]. The pressure curve according to Hertz (green), the hydrodynamic pressure curve (red) and the temperature distribution (blue) occurring in the lubrication gap are illustrated. Due to its relevance with regard to the load carrying capacity of gears, especially the tribologically affected damage types micropitting and wear, the focus of the analysis is predominantly on the minimum lubricant film thickness h_m and the (maximum) contact temperature θ_B in the TEHL contact.

3.2 Simulation model

For the theoretical investigations, a TEHL simulation model called TriboMesh acc. to Lohner et al. [13] and Ziegltrum et al. [24, 25] is applied. The TEHL simulation model is based on a full-system approach, which a discretized overall calculation area is defined on the basis of rolling elements and lubricating film for. The solution scheme of TriboMesh includes three successive levels of detail. To define the contact conditions, all parameters, such as lubricant and solid properties (incl. adequate lubricant model approaches), operating conditions and numerical inputs are set within the initialization. An initial calculation is performed to determine the pressure and lubricant film thickness profile of an isothermal EHL contact with Newtonian lubricant behavior. The solution of this calculation step serves as a starting

Fig. 4 Contraform TEHL contact of two convex contact bodies, acc. to [6] cited in [18]
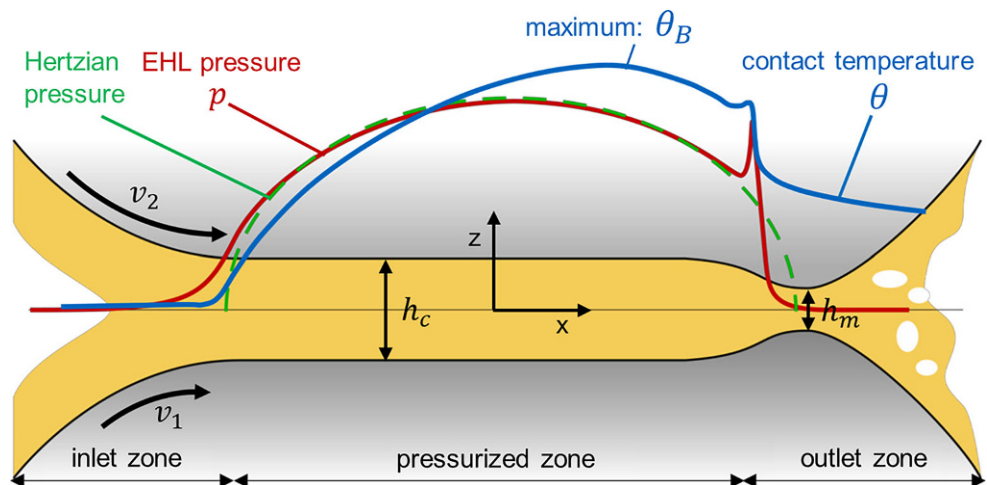
value for the following calculation of an isothermal EHL contact with non-Newtonian lubricant behavior. Here, in addition to the lubricant film thickness and the pressure distribution, the shear stress in the lubricant is also calculated. In the third calculation step, the elastohydrodynamic temperature distribution is calculated coupled iteratively. Finally, the results have been prepared in a subsequent post-processing step. Consequently, the results (lubricant film thickness and contact temperature) shown in the following are based on numerical simulations under consideration of non-Newtonian lubricant behavior and thermal effects [13].

For the theoretical studies presented within this paper, calculations with stationary operating behavior are performed in selected contact points of the path of contact (A: start of contact, B: inner single contact point, C: pitch point, M: center of active profile [for variants C below and C above], D: outer single contact point, E: end of contact). It is to be noted that for the contact points B, M and D but also for the (depending on the variant partially virtual) pitch point C, single tooth contact is considered in the simulation. As only spur gear geometries are part of the investigations, the TEHL simulation model is applied as 2-dimensional system. Fully smooth surfaces are assumed and therefore, no mixed lubrication is considered. As input parameters serve the pressure and the speed conditions in each selected contact point for an uncorrected gear geometry (no flank modifications considered) as well as the bulk temperature ϑ_M according to Oster [16] (see Eq. 3)[1].

$$\vartheta_M = \vartheta_{\text{oil}} + 7400 \cdot \left(\frac{P \cdot \mu_{mz} \cdot H_V}{|a| \cdot b} \right)^{0.72} \cdot \frac{X_S}{1.2 \cdot X_{Ca}}. \quad (3)$$

Here, the mean coefficient of friction μ_{mz} is calculated according to Schlenk [21] (see Eq. 4)[1], while an average surface roughness of $Ra = 0.3\,\mu m$ is considered.

$$\mu_{mz} = 0.048 \cdot \left(\frac{\frac{F_{bt}}{b}}{v_{\Sigma C} \cdot \rho_{\text{redC}}} \right)^2 \cdot \eta_{\text{oil}}^{-0.05} \cdot Ra^{0.25} \cdot X_L. \quad (4)$$

The tooth loss factor H_V is determined by the extended approach according to Wimmer [23] (see Eq. 5)[1], where the position of the pitch point can also be taken into account for gear geometries with C outside of the active profile.

$$H_V = \frac{\pi \cdot (u + 1)}{z_2} \cdot (a_0 + a_1 |\varepsilon_1| + a_2 |\varepsilon_2| + a_3 |\varepsilon_1| \varepsilon_1 + a_4 |\varepsilon_2| \varepsilon_2). \quad (5)$$

[1] *Note*: Nomenclature and detailed explanations considering Eq. 3–5 are to be found in the original literature [16, 21, 23]

4 Results of the simulation study

In the following, the minimum lubricant film thickness h_m and the (maximum) contact temperature θ_B determined by TEHL simulation (see Chap. 3) are presented. To show the influence of the loading and the circumferential speed, different operating conditions are considered within the numerical TEHL calculations (see Chap. 2.3) for the investigated gear geometries (see Chap. 2.1 and 2.2). The results are mainly based on the work within [18, 19].

4.1 Minimum lubricant film thickness

Within Fig. 5 (left), the influence of the load stage (BS 6–11, with $v_t = \text{const.} = 2.0\,\text{m/s}$) is illustrated.

For all geometries, the minimum of h_m over the active profile can be found in the beginning of contact (point A), which is characterized by double tooth contact. A clear decrease of h_m can be observed with increased load stage in all investigated contact points, where the absolute differences become greater in the direction of the end of contact (point E).

The reference geometry shows in point A with $h_{m,A} \approx 0.03$–$0.07\,\mu m$ the smallest values and also the smallest differences for the different load stages compared to the variants C below ($h_{m,A} \approx 0.05$–$0.13\,\mu m$) and C above ($h_{m,A} \approx 0.07$–$0.15\,\mu m$). h_m increases over the active profile, partially up to approx. $10 \cdot h_{m,A}$. Variant Ref is also characterized by the highest values in point E since the active profile length is significantly increased in comparison to the other variants.

On the right side of Fig. 5, the influence of the circumferential speed ($v_t = 2.0$, 0.5 and 0.05 m/s at BS 6) is shown for each gear geometry. The simulation points present a clear decrease of h_m with reduced circumferential speeds in all investigated contact points, the absolute differences show for each geometry a maximum in point E. For the slowest circumferential speed ($v_t = 0.05\,\text{m/s}$), the difference between beginning (A) and end (E) of contact is less significant, comparable values ($h_{m,A} \approx 0.01$–$0.02\,\mu m$, $h_{m,E} \approx 0.04\,\mu m$) are specified for all variants.

All in all, the results of the simulation study confirm the basic analytical relations between the minimum lubricant film thickness h_m and the influence parameters load respectively circumferential speed v_t according to [5] for internal gears with balanced, but also unbalanced sliding conditions.

Within former research [10, 11, 22] on the reference geometry, it was shown that the defined operating conditions are adequate to investigate the micropitting and wear behavior of internal gears. As a good comparability of h_m can be seen (especially with more critical conditions at higher load stages respectively lower circumferential speeds), it can be assumed that the three designed gear geometries are suitable to investigate the influence of unbalanced sliding

Fig. 5 Local minimum lubricant film thickness h_m within the active profile determined by TEHL simulation (*left*: influence of the load stage with $v_t = \text{const.} = 2.0$ m/s, *right*: influence of the circumferential speed at BS 6)
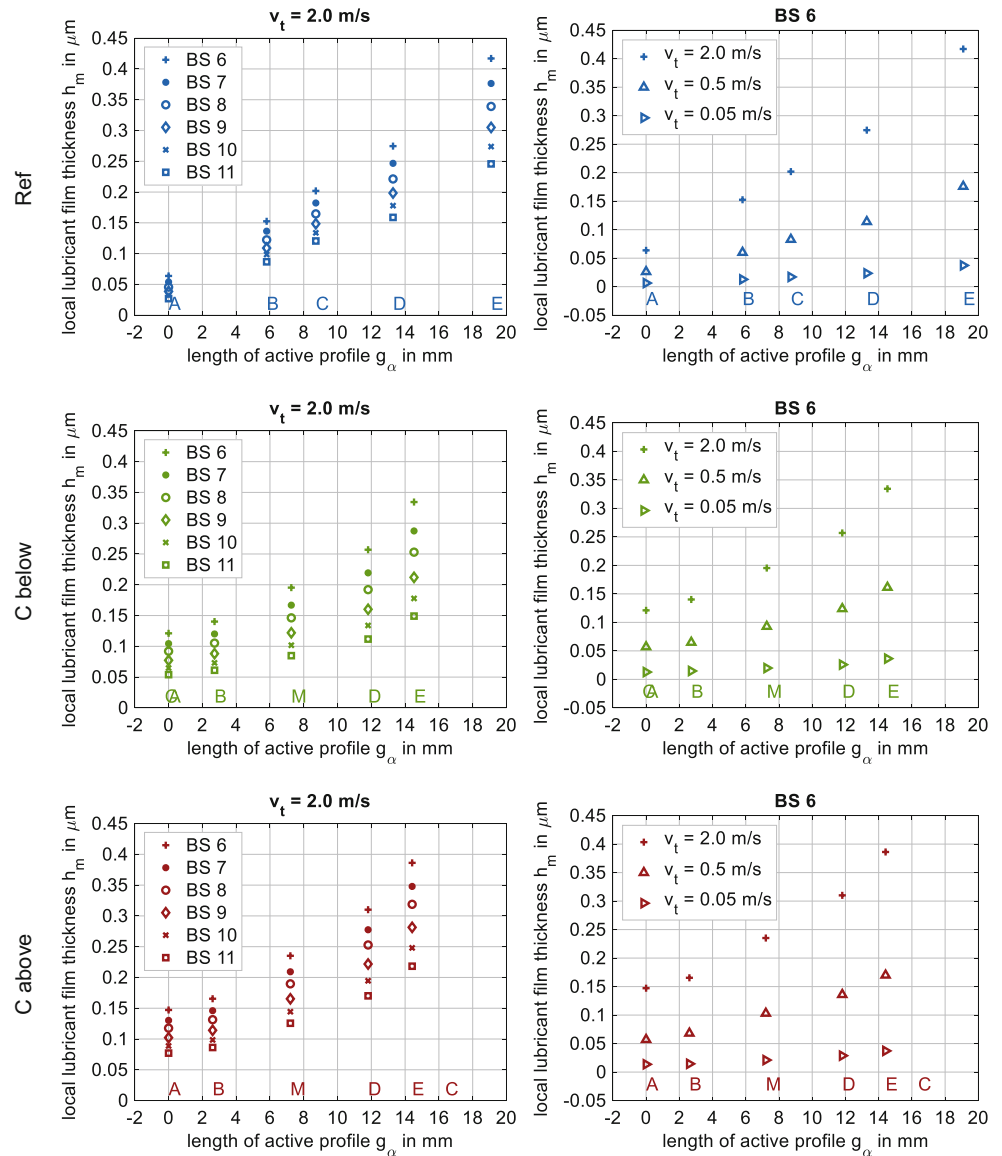

4.2 Contact temperature

The simulations confirm that the smallest values (and also the smallest differences) of the contact temperature θ_B can be found in or near the pitch point C (see Fig. 6) where no or the minimum sliding speeds in the tooth contact occur. The values correspond here approx. to the bulk temperature ϑ_M (input parameter of the simulation). Consequently, beginning (A) respectively end (E) of contact are characterized by the minimum of θ_B for variant C below respectively C above. The highest values of θ_B are observed in point A for the reference, point D for variant C below and point B for C above, where the most crucial conditions combined regarding pressure and sliding speed can be assumed.

conditions on the flank load carrying capacity within experimental investigations.

Fig. 6 (left) shows that the contact temperature θ_B increases for higher load stages. The maximum values are almost comparable for the reference ($\theta_{B,A} \approx 83\text{–}119\,°\text{C}$), variant C below ($\theta_{B,D} \approx 88\text{–}127\,°\text{C}$) and C above ($\theta_{B,B} \approx 88\text{–}122\,°\text{C}$).

The data illustrate also the significant decreasing influence of reduced circumferential speeds on the contact temperature θ_B (see Fig. 6, right). Especially for the simulation with the slowest circumferential speed ($v_t = 0.05$ m/s), only a marginal difference over the active profile can be observed, all geometries show comparable values slightly $>60\,°\text{C}$.

Fig. 6 Contact temperature θ_B within the active profile determined by TEHL simulation (*left*: influence of the load stage with $v_t = \text{const.} = 2.0\,\text{m/s}$, *right*: influence of the circumferential speed at BS 6)
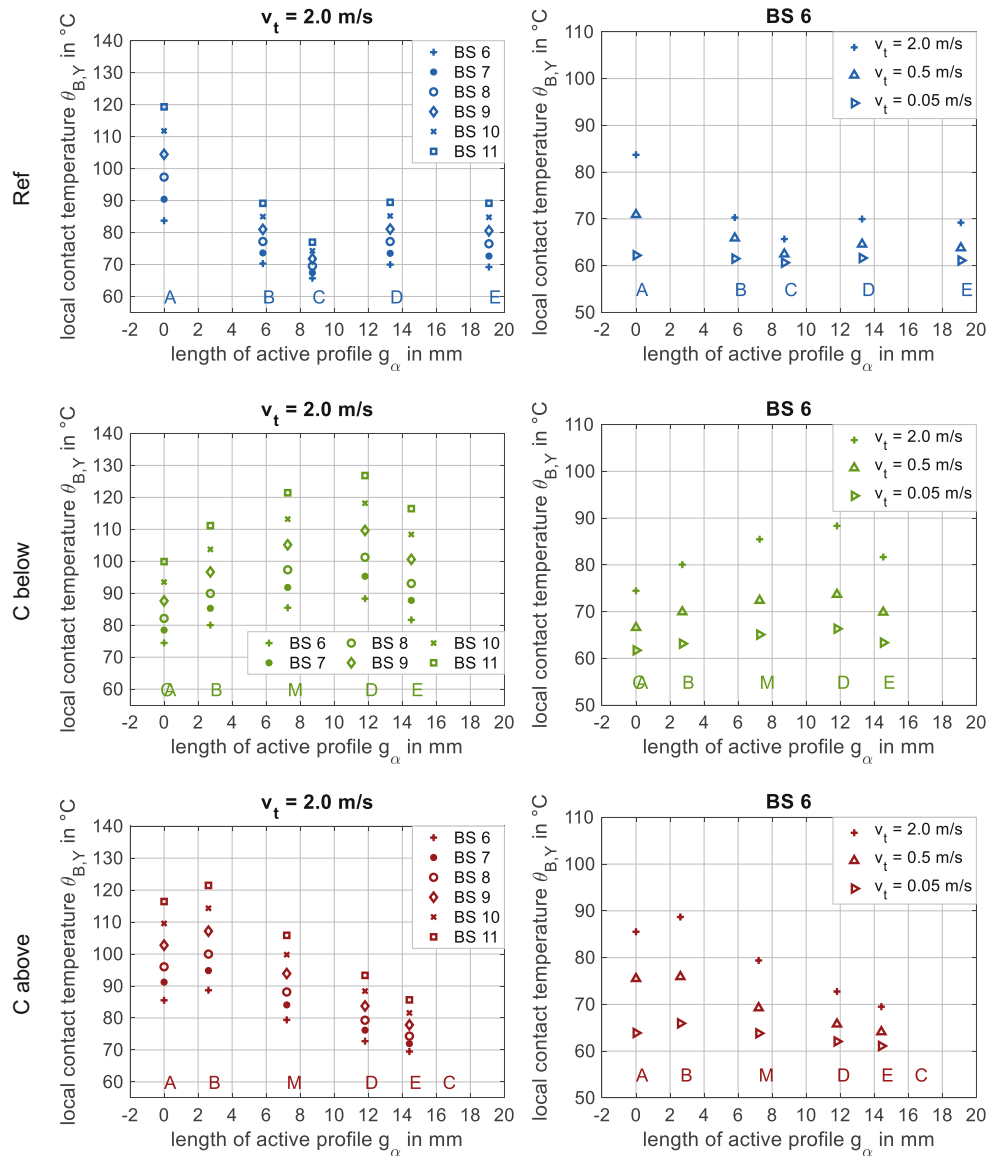
5 Comparison to analytical approaches in the load carrying capacity calculation of gears

As the minimum lubricant film thickness h_m plays a decisive role within the micropitting load capacity calculation acc. to ISO/TS 6336-22 [2] (only valid for external gears) and wear calculation acc. to Plewe [17], an exeplary comparison of the simulation results and each analytical approach, which is mainly based on [5], is shown in the following.

5.1 Micropitting load capacity calculation acc. to ISO/TS 6336-22

Fig. 7 illustrates the determined local minimum lubricant film thickness h_m (left) and the contact temperature θ_B (right) over the active profile from the numerical TEHL sim-

ulation and the analytical calculation according to ISO/TS 6336-22 [2] for the operating conditions $v_t = 2.0\,\text{m/s}$ at BS 6.

Generally, a good comparability of h_m can be observed for all three geometries (see Fig. 7, left). From the analytical approach, slightly decreased values result, which would be estimated more on the conservative side. Especially in the critical contact points of the active profile (note: according to ISO/TS 6336-22 [2], the minimum of the specific minimum lubricant film thickness $\lambda = h_m/Ra$ in the area of negative specific sliding is considered for the micropitting load capacity calculation), the values of numerical simulation and analytical calculation show a fairly good comparability.

However, it is to be added in this context that the target of the analytical method according to ISO/TS 6336-22 [2] is less to estimate a highly "correct" absolute value of the lu-
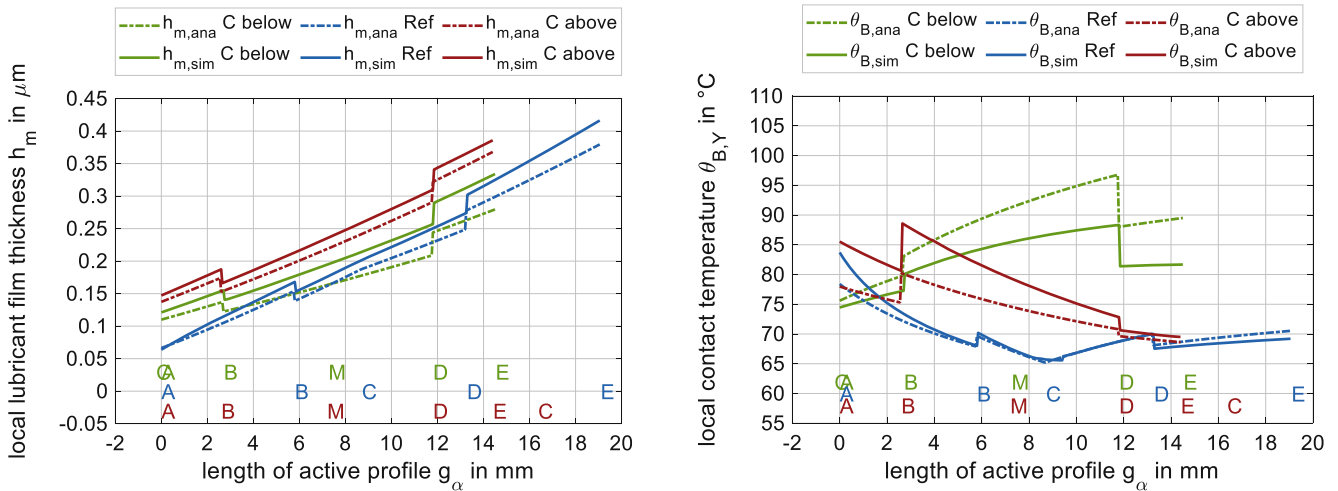
Fig. 7 Comparison of the local minimum lubricant film thickness h_m (*left*) and the contact temperature θ_B (*right*) determined by TEHL simulation and analytical calculation acc. to ISO/TS 6336-22 [2] for $v_t = 2.0$ m/s at BS 6

bricant film thickness. Rather, the micropitting load capacity is determined based on safety factor S_λ by a comparison between the determined occurring and a permissible specific lubricant film thickness (calculated from testing with standardized test gears [1, 8]). Consequently, differences due to other uncertainties or assumptions of numerical and analytical approach would be eliminated within the micropitting load capacity calculation method, when both occurring and permissible film thickness are based on the same approach.

Regarding the contact temperature (see Fig. 7, right), a good correspondence between simulation and analytical calculation in the area near the pitch point C can be detected. Both methods result in comparable curve trends, the differences (mainly in areas with greater distance from pitch point C) are for the presented conditions in most of the active profile in a range of $< 5\,°C$. Analytically, decreased values of the contact temperature are calculated in areas of negative specific sliding on the planet flank (resp. positive specific sliding on the ring gear flank, see i.e. variant C above) compared to the simulation. In contrast, the analytical calculation leads to increased values in areas of positive specific sliding on the planet flank (resp. negative specific sliding on the ring gear flank, see i.e. variant C below). Consequently, a dependency of the deviations on the sliding direction is probable. Since such a systematic relation was not observed for the differences of the lubricant film thickness, the alternating temperatures between simulation and analytical calculation are assumed to have only a partial responsibility on the deviations of h_m.

5.2 Wear calculation acc. to Plewe

A comparison of the minimum lubricant film thickness based on the TEHL simulation and the analytical calculation approach according to Plewe [17], where only the pitch point C is considered, is shown in Fig. 8 by $\Delta h_{abs,C} = h_{m,C|Plewe} - h_{m,C|sim}$ resp. $\Delta h_{rel,C} = \Delta h_{abs,C} / h_{m,C|Plewe}$. It should be noted that for the calculations in the virtual pitch point of the C below and C above variants, the contact conditions were assumed taking into account a single tooth contact. It can be seen that lower values of $h_{m,C}$ for variants Ref and C below respectively increased values for variant C above are determined by TEHL simulation compared to the analytical calculation. For all gear geometries, generally smaller absolute differences can be observed at lower circumferential speeds respectively higher flank pressures (see Fig. 8, above). Especially for wear-critical conditions (low circumferential speeds combined with high flank pressures), very small deviations can be observed. Only at higher circumferential speeds and low flank pressures, larger absolute deviations between simulation and analytical calculation are present, i.e. under conditions where (at least for the considered material pairing at hand) no wear is usually to be expected. The relative deviation $\Delta h_{rel,C}$ (see Fig. 8, below) shows a comparably constant level for each variant, the average is determined with approx. +23% (Ref), +24% (C below) and –5% (C above).

However, mainly for the variants C below and C above, further (experimental) investigations are necessary analyzing to what extent the calculated values of the minimum lubricant film thickness at the pitch point C, which is not part of the active profile, are representative for an estimation of the wear resistance according to Plewe. A local wear

Fig. 8 Difference $\Delta h_{abs,C}$ (*above*) resp. $\Delta h_{rel,C}$ (*below*) of the minimum lubricant film thickness at the pitch point C determined by TEHL simulation and analytical calculation acc. to Plewe [17] for different conditions
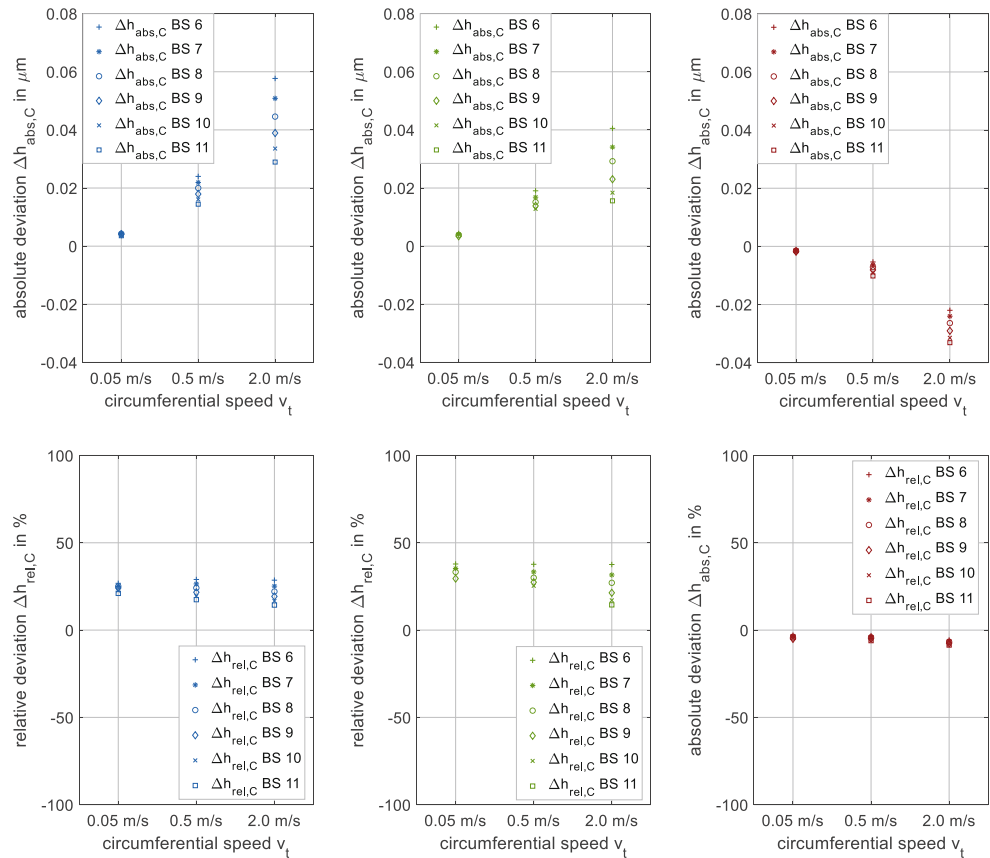
calculation method (see [20]) may be preferable for gears with unbalanced sliding conditions.

6 Further considerations on calculation of the coefficient of friction for gears with unbalanced sliding conditions

In the comparison between contact temperatures calculated analytically according to ISO/TS 6336-22 [2] and those simulated using the TEHL model TriboMesh, partly more significant differences (depending on the operating conditions) could be identified. The differences in the contact temperature are assumed to be at least partially responsible for different values of the lubricant film thickness in analytical calculation and simulation (see Chap. 5.1).

The considered coefficient of friction has a corresponding influence on the bulk and flash temperatures in analytical calculations. Since the mean coefficient of friction μ_{mz} according to both Michaelis [15] (in ISO/TS 6336-22 [2]) and Schlenk [21] is calculated for the contact conditions in the pitch point C, such a calculation for the variants C below and C above (where C only represents a virtual contact point) is not representative for the friction conditions of the active profile.

Exemplarily, Fig. 9 shows a calculation of the mean coefficient of friction with the corresponding equations from [2, 15] for the conditions in the center M of the active profile. For variant C below, μ_{mz} in contact point M is reduced compared with the original determination according to ISO/TS 6336-22 [2] in pitch point C, while a higher value was calculated for variant C above. The adjusted coefficient of friction would lead to a certain approximation of the results from analytical calculation and simulation, especially in active profile zones with larger distance from the pitch point.

However, available approaches for determining the mean coefficient of friction for gears are derived and validated exclusively from investigations on external gear geometries, the application to internal gears remains to be checked. Ap-

	Ref	C below	C above
μ_{mz} in C	0.047	0.062	0.032
μ_{mz} in M	0.045	0.040	0.044
$\Delta\mu_m$	- 4 %	- 35 %	+ 38 %

Fig. 9 Exemplarily calculated coefficients of friction in different contact points (C, M) acc. to equation from ISO/TS 6336-22 [2, 15] (BS 6 and $v_t = 2.0$ m/s)

proaches for the local gear coefficient of friction also need to be validated. In this context, it is to be noted that the friction behavior and efficiency determination of internal gears are part of current research at FZG within comprehensive theoretical and experimental investigations.

7 Conclusion and outlook

Extended theoretical studies on the tribological characteristics of different internal gear designs have been presented within this paper. A reference geometry with balanced sliding conditions was compared to internal gears with pitch point C below respectively above the active profile. Based on existing experimental test methods [1, 8, 22], comparable conditions for the different gear designs have been defined with unbalanced sliding conditions using FZG calculation software RIKOR [7]. Due to its relevance with regard to the load carrying capacity of gears, especially the tribologically affected damage types micropitting and wear, the focus of the analysis was predominantly on the minimum lubricant film thickness h_m and the contact temperature θ_B. Therefore, systematic numerical calculations using the TEHL simulation model TriboMesh [12, 24, 25] applied to the three gear designs have been performed.

All in all, the results of the simulation study confirm the basic analytical relations according to [5] for internal gears with balanced, but also unbalanced sliding conditions. Within former research [10, 11, 22], it was shown that the defined operating conditions on the reference geometry are adequate to investigate the micropitting and wear behavior of internal gears. As a good comparability could be seen (especially with more critical conditions at higher load stages respectively lower circumferential speeds), it can be assumed that the designed gear geometries with pitch point C outside of the active profile are suitable to investigate the influence of unbalanced sliding conditions on the flank load carrying capacity within experimental investigations.

The simulation results have been compared to the analytical approaches according to ISO/TS 6336-22 [2] and Plewe [17] in the context of the calculation of load carrying capacity. It could be seen that especially in the critical contact points of the active profile respectively for critical conditions (low circumferential speeds, high flank pressures) considering micropitting and wear, the values of numerical simulation and analytical calculation show a fairly good comparability. As numerous existing calculation approaches mainly consider the conditions in the pitch point C (e.g. lubricant film thickness acc. to [17] or mean coefficient of friction acc. to [15, 21]) , it was shown that further (experimental) investigations are necessary analyzing to what extent the calculated values are representative for gears with unbalanced sliding condition. Therefore, local calculation methods may be preferable for such gear designs.

Within experimental investigations on internal gears including the designed gear geometries with unbalanced sliding conditions, the effects of the specific sliding on the pitting (comparably to [9]), micropitting and wear load carrying capacity as well as efficiency is part of current research at FZG.

References

1. DIN 3990-16:2020: Tragfähigkeitsberechnung von Stirnrädern – Teil 16: Bestimmung der Grauflecken-tragfähigkeit von Schmierstoffen im FZG-Prüfverfahren GT-C/8,3/90 [engl.: Calculation of load capacity of cylindrical gears—Part 16: Determination of the micro-pitting load-carrying capacity of lubricants using FZG-test-method GT-C/8,3/90] (2020).
2. ISO/TS 6336-22:2018-08: Calculation of load capacity of spur and helical gears—Part 22: Calculation of micropitting load capacity (2018).
3. ISO 6336-1:2019-11: Calculation of load capacity of spur and helical gears—Part 1: Basic principles, introduction and general influence factors (2019).
4. Bartel D (2010) Simulation von Tribosystemen – Grundlagen und Anwendungen
5. Dowson D, Higginson GR (1977) Elasto-hydrodynamic lubrication. Pergamon Press, Oxford, New York
6. Ebner M, Yilmaz M, Lohner T, Michaelis K, Höhn B-R, Stahl K (2015) On the effect of starved lubrication on elastohydrodynamic (EHL) line contacts. Tribol Int 118:515–523
7. Gear Research Center (FZG) Technical University of Munich: Simulation and Computer Programs. https://www.mec.ed.tum.de/en/fzg/research/simulation-and-computer-programs/. Accessed 1 Mar 2023
8. Forschungsvereinigung Antriebstechnik e. V. (1993) Information Sheet 54/7 Micropitting—Test procedure for the investigation of the micro-pitting capacity of gear lubricants

9. Geitner M, Zornek B, Tobie T, Stahl K (2019) Investigations on the pitting load capacity of internal spur and helical gears. Forsch Ingenieurwes 83:553–561

10. Geitner M, Zornek B, Hoja S, Tobie T, Stahl K (2021) Investigations on the micro-pitting and wear behavior of Nitrided internal gears. IOP Conf Ser: Mater Sci Eng 1097:12005

11. Höhn B-R, Stahl K, Schudy J, Tobie T, Zornek B (2011) Investigations on the flank load carrying capacity in the newly developed FZG back-to-back test rig for internal gears. 2011 Fall Technical Meeting (FTM). American Gear Manufacturers Association, Cincinnati

12. Lohner T (2016) Berechnung von TEHD Kontakten und Einlaufverhalten von Verzahnungen. PhD Thesis, Technical University of Munich

13. Lohner T, Zie05trum A, Stemplinger J-P, Stahl K (2016) Engineering software solution for thermal elastohydrodynamic lubrication using multiphysics software. Adv Tribol. https://doi.org/10.1155/2016/6507203

14. Mayer J (2013) Einfluss der Oberfläche und des Schmierstoffs auf das Reibungsverhalten im EHD-Kontakt. PhD Thesis, Technical University of Munich (2013)

15. Michaelis K (1987) Die Integraltemperatur zur Beurteilung der Fresstragfähigkeit von Stirnradgetrieben. PhD Thesis, Technical University of Munich

16. Oster P (1982) Beanspruchung der Zahnflanken unter Bedingungen der Elastohydrodynamik. PhD Thesis, Technical University of Munich

17. Plewe H.-J (1980) Untersuchung über den Abriebsverschleiß von geschmierten, langsam laufenden Zahnrädern. PhD Thesis, Technical University of Munich

18. Preintner S (2021) TEHD-Simulation von tribologisch optimierten Innenverzahnungen. Semester Thesis, Technical University of Munich

19. Preintner S (2022) Untersuchungen zum Graufleckenverhalten tribologisch optimierter Innenverzahnungen. Master's Thesis, Technical University of Munich

20. Schudy J (2010) Untersuchungen zur Flankentragfähigkeit von Außen- und Innenverzahnungen – Einflüsse auf das Grübchen-, Grauflecken- und Verschleißverhalten, insbesondere bei langsam laufenden Getriebestufen. PhD Thesis, Technical University of Munich

21. Schlenk L (1995) Untersuchungen zur Freßtragfähigkeit von Großzahnrädern. PhD Thesis, Technical University of Munich

22. Stahl K, Höhn B-R, Schudy J, Tobie T, Zornek B (2013) Investigations on the flank load carrying capacity of internal gears. International Conference on Gears 2013. VDI – Verein Deutscher Ingenieure, München

23. Wimmer AJ (2005) Lastverluste von Stirnradverzahnungen – Konstruktive Einflüsse, Wirkungsgradmaximierung, Tribologie. PhD Thesis, Technical University of Munich

24. Zie05trum A, Lohner T, Stahl K (2016) TEHL simulation on the influence of lubricants on load-dependent gear losses. Tribol Int 113:252–261

25. Zie05trum A, Lohner T, Stahl K (2018) TEHL simulation on the influence of lubricants on the frictional losses of DLC coated gears. Lubricants 6(1):1–17

26. Zornek B (2018) Untersuchungen zur Flankentragfähigkeit vergüteter und nitrierter Innen- und Außenverzahnungen. PhD Thesis, Technical University of Munich